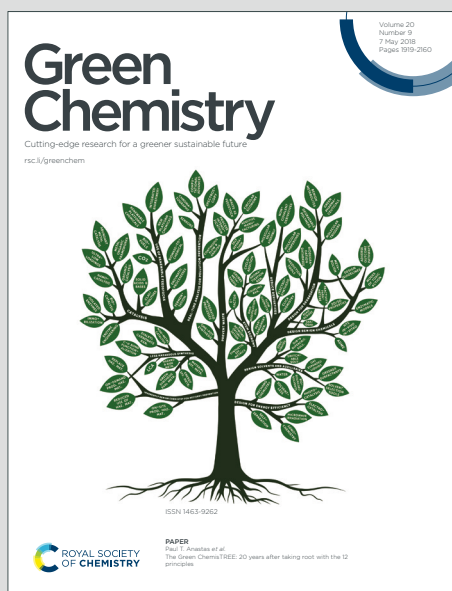


Green Chemistry

Cutting-edge research for a greener sustainable future

Accepted Manuscript

This article can be cited before page numbers have been issued, to do this please use: L. Jiang, J. Ming, L. Wang, Y. Jiang, L. Ren, Z. Wang and W. Cheng, *Green Chem.*, 2020, DOI: 10.1039/C9GC03727F.



This is an Accepted Manuscript, which has been through the Royal Society of Chemistry peer review process and has been accepted for publication.

Accepted Manuscripts are published online shortly after acceptance, before technical editing, formatting and proof reading. Using this free service, authors can make their results available to the community, in citable form, before we publish the edited article. We will replace this Accepted Manuscript with the edited and formatted Advance Article as soon as it is available.

You can find more information about Accepted Manuscripts in the [Information for Authors](#).

Please note that technical editing may introduce minor changes to the text and/or graphics, which may alter content. The journal's standard [Terms & Conditions](#) and the [Ethical guidelines](#) still apply. In no event shall the Royal Society of Chemistry be held responsible for any errors or omissions in this Accepted Manuscript or any consequences arising from the use of any information it contains.

COMMUNICATION

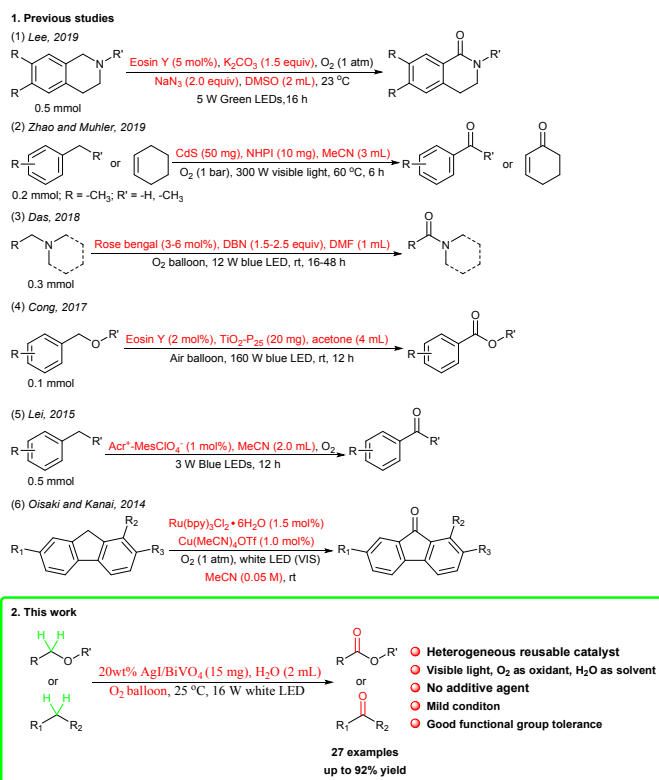
Visible-Light-Induced Selective Aerobic Oxidation of sp^3 C-H bonds Catalyzed by Heterogeneous AgI/BiVO₄ catalystReceived 00th January 20xx,
Accepted 00th January 20xxLi-ya Jiang,^{a, c} Jing-jing Ming,^{a, c} Lian-Yue Wang,^b Yuan-yuan Jiang,^a Lan-hui Ren,^{a, *} Zi-cheng Wang,^a Wen-chen Cheng^a

DOI: 10.1039/x0xx00000x

An efficient oxidation of sp^3 C-H bonds to esters and ketones has been developed using AgI/BiVO₄ as photocatalyst and O₂ as oxidant in water. Various substrates can be transformed into the desired esters and ketones in moderate to good yields. The synthetic utility of this approach has been demonstrated by gram-level experiments and consecutive oxidation experiments. A plausible mechanism has been proposed.

Oxygen-bearing groups (hydroxyl and carbonyl) are important structures found in many bioactive molecules and pharmaceutical agents, such as apromidine, pheniramine, chlorpheniramine, triprolidine, doxylamine, isochromanones, etc.¹ The direct oxidation of the sp^3 C-H bonds is an attractive way to construct oxygen-bearing groups. Traditionally, stoichiometric quantities of hazardous oxidants, such as high-valent metal salts, halides and peroxides, were used for these chemical transformations resulting in large amounts of unwanted by-products.² Therefore, development of cleaner and cost-effective methodology for the oxidation of sp^3 C-H bonds is highly important and significant.

Direct oxidation of the sp^3 C-H bonds using environmentally benign oxidants (O₂ or air) under mild conditions offers straightforward access to oxygen-bearing groups formation which has advantages of easy accessible raw materials, H₂O as by-product, high atom economy over the alternative stoichiometric oxidation protocols. However, owing to the triplet ground state structure, molecule oxygen is relatively inert under mild conditions, especially towards inert C-H bonds. Although the oxidation of the sp^3 C-H bonds forming oxygen-bearing groups using molecular oxygen has been studied, to this day, many promising results were obtained using transition-metal catalysts³⁻⁸ or non-metal catalysts⁹ under relatively harsh



Scheme 1. Visible-light-induced photocatalytic oxidation of the sp^3 C-H bonds using O₂ or air as oxidants.

conditions (high temperature and pressure). Thus, the development of simple and mild methods for selective oxidation of the sp^3 C-H bonds is highly desirable.

Due to its ecocompatibility, easy availability, safe handling and everlasting abundance as an energy source, visible-light has received central attentions from various research groups. Visible-light-induced photocatalysis have been developed into powerful tools for the functionalization of organic molecules under mild conditions.¹⁰ The molecular oxygen had been used as oxidant in many visible-light-induced catalytic oxidation of the sp^3 C-H bonds. Many exciting results were obtained

^a College of Pharmacy, Weifang Medical University, Weifang 261053, P. R. China; E-mail: Ren_lanhui@163.com.

^b Dalian Institute of Chemical Physics, the Chinese Academy of Sciences and Dalian National Laboratory for Clean Energy, DNL, 457 Zhongshan Road, Dalian, 116023, P. R. China.

^c Li-ya Jiang and Jing-jing Ming contributed equally to this work.

Electronic Supplementary Information (ESI) available. See DOI: 10.1039/x0xx00000x

involving semiconductors or organic dyes or organic small molecules photocatalytic oxidation systems, such as eosin Y/K₂CO₃/NaN₃,^{11a} CdS/NHPI,^{11b} DDQ/TBN/AcOH,^{11c} 11h hydroquinone/CuCl₂ • 6H₂O,^{11d} rose bengal/DBN,^{11e} eosin Y/TiO₂-P₂₅,^{11f} CBr₄,^{11g} riboflavin tetraacetate (RFT)/Fe complex,¹¹ⁱ 9-mesityl-10-methylacridinium ion (Acr⁺-MesClO₄⁻),^{11j} 2-chloroanthraquinone (2-Cl-AQN),^{11k} Ru(bpy)₃Cl₂ • 6H₂O/Cu(MeCN)₄OTf^{11l} and g-C₃N₄/NHPI.^{11m} Some photocatalytic oxidation systems are listed in Scheme 1-1.

For years, we have been studying the clean oxidation of the *sp*³ C-H bonds, and we have reported eco-friendly protocols for the oxidation of the *sp*³ C-H bonds adjacent to pyridine moiety.^{9h, 12} In line with our ongoing interest in green chemistry and uninterrupted studies on the selective aerobic oxidation of *sp*³ C-H bonds, herein, we present an efficient oxidation of *sp*³ C-H bonds to esters and ketones (Scheme 1-2). This transformation features a visible-light-induced heterogeneous reusable AgI/BiVO₄ catalyzed reaction with O₂ as green oxidant and H₂O as solvent. The white LED lamp bought from market is used as light source. Notably, this transformation do not require any additive. This method is efficient and applicable to a broad range of substrates with good functional group compatibility.

As we know, many visible-light-induced catalytic oxidation of the *sp*³ C-H bonds that the oxidant is molecular oxygen involve superoxide radical anion (O₂^{•-}).¹¹ According to the literature,¹³ AgI/BiVO₄ was excited by visible light to generate the photoelectrons which could reduce the dissolved molecular oxygen on the surface of the AgI/BiVO₄ material forming O₂^{•-}. O₂^{•-} could damage cell walls and resulted in antimicrobial effects.

We envisioned that the oxidation of the *sp*³ C-H bonds might be accomplished via a visible-light-induced process using AgI/BiVO₄ as catalyst and molecular oxygen as oxidant. In an effort to test this hypothesis, AgI/BiVO₄ materials were prepared by an *in situ* deposition-precipitation procedure (see Supporting Information) reported in the literature.¹⁴ Scanning electron microscope (SEM), transmission electron microscope (TEM), X-ray diffraction (XRD) and X-ray photoelectron spectroscopy (XPS) were used for characterizing the AgI/BiVO₄ materials (Figure 1-3). The morphological evolution of 20wt% AgI/BiVO₄ material was examined by SEM (Figure 1A and 1B) and TEM (Figure 1C and 1D) analysis. Both two types of morphologies (AgI and BiVO₄) were found in 20wt% AgI/BiVO₄ nanocomposite. A large number of irregular AgI nanoparticles distributed on the surface of BiVO₄, indicating that AgI and BiVO₄ were well combined with each other. The sizes of AgI particles were about 13.08-95.94 nm. The length of BiVO₄ particles were about 1.03-2.06 μm, and the width were about 0.15-0.77 μm.

The phase compositions of pure AgI, pure BiVO₄ and 20wt% AgI/BiVO₄ were characterized by X-ray diffraction (XRD). As showed in Figure 2, the peaks of BiVO₄ at 2θ values of 18.61°, 28.90°, 30.56°, 35.24°, 39.80°, 42.50°, 45.37°, 46.73°, 49.89°, 53.36°, 55.27° and 59.27° could be attributed to (011), (121), (040), (002), (211), (051), (231), (240), (202), (161), (321) and (123) crystal planes of BiVO₄ (JCPDS File No. 14-0688), respectively. The characteristic peaks of AgI were ascribed to

hexagonal β-AgI (JCPDS File No. 09-0374). The XRD spectra of 20wt% AgI/BiVO₄ presented a good coexistence of AgI and BiVO₄. The result showed that AgI was successfully introduced into the BiVO₄ systems.¹⁴

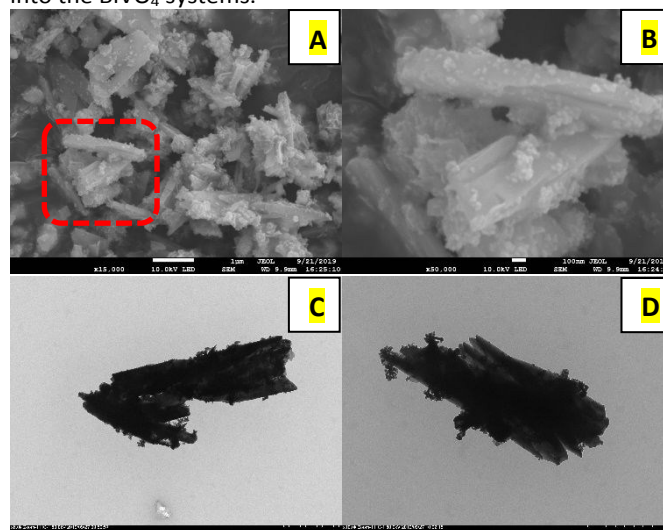


Figure 1. SEM (A and B) and TEM (C and D) images of the 20wt% AgI/BiVO₄.

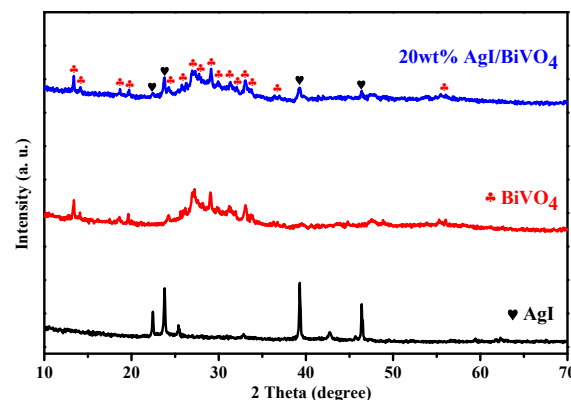


Figure 2. The XRD patterns of pure AgI, pure BiVO₄ and 20wt% AgI/BiVO₄.

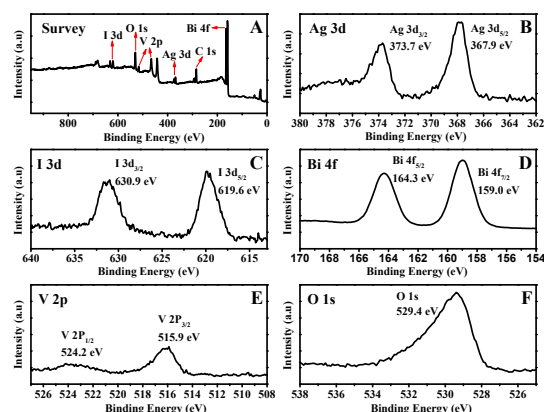


Figure 3. The XPS spectra of 20wt% AgI/BiVO₄ sample: (A) survey scan, (B) Ag 3d, (C) I 3d, (D) Bi 4f, (E) V 2p and (F) O 1s.

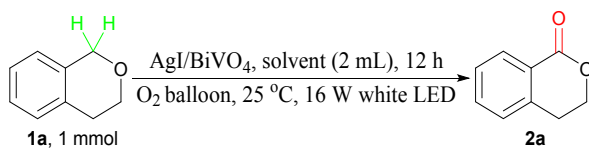
The survey XPS spectrum of 20wt% AgI/BiVO₄ (Figure 3A) showed that the predominant elements of the samples were C, Bi, V, O, Ag and I. The carbon element was ascribed to the adventitious hydrocarbons from the XPS instrument itself. In the XPS spectrum of Ag 3d, two peaks were observed at 367.9

and 373.3 eV, which originated respectively from Ag 3d_{5/2} and Ag 3d_{3/2} (Figure 3B). The two peaks could not be divided into four peaks, indicating only the existence of Ag⁺ among AgI/BiVO₄ composites. Figure 3C presented that the high-resolution XPS spectrum of I 3d, the peaks appeared at binding energy (BE) of 619.6 and 630.9 eV were ascribed to I 3d_{5/2} and I 3d_{3/2}, respectively. The peaks located at 159.0 and 164.3 eV were belonged to Bi 4f_{7/2} and Bi 4f_{5/2} (Figure 3D), respectively. Two obvious peaks situated at banding energies of 515.9 and 524.2 eV were clearly perceived in Figure 3E, which should belong to V 2p_{3/2} and V 2p_{1/2}, respectively. The peaks at 529.4 eV in Figure 3F were attributed to O 1s. The XPS results were further to confirm the successful combination of BiVO₄ and AgI.^{13, 14}

We employed commercially isochroman (**1a**) as model substrate in the presence of 10 mg 20wt% AgI/BiVO₄ using MeCN as solvent in O₂ atmosphere under a 16 W white LED at 25 °C for 12 h, giving the desired product (1-isochromanone, **2a**) in 28% yield (Table 1, entry 1). No desired product was observed with neither AgI/BiVO₄ nor light which indicated that the AgI/BiVO₄ and light were essential to this process (Table 1, entries 2 and 3). The reaction did not happen in the absence of O₂ (Table 1, entry 4). Various reaction parameters were tested in oxygen atmosphere under a 16 W white LED at 25 °C for the optimization of reaction parameters including solvents, catalysts, and reaction time to identify the optimal reactions conditions. First, as shown in Table 1, different solvents, such as H₂O, EtOH, MeOH, CH₂Cl₂, toluene, N, N-dimethylformamide (DMF), 1,4-dioxane and 1,2-dichloroethane (DCE) were screened, yielding 1-isochromanone (**2a**) in 78%, 35%, 10%, 16%, 18%, 5%, 16% and 33% isolated yields, respectively (Table 1, entries 5-12). This oxidation reaction did not occur in ethyl acetate (EA) (Table 1, entry 13). H₂O was found to be more effective for this transformation which might be because the water-insoluble characteristic of isochroman led to its concentration on the surface of heterogeneous AgI/BiVO₄ catalyst. Therefore, H₂O was the best choice for the next optimization study. Next, a survey of different AgI/BiVO₄ catalysts (different AgI contents) was carried out, revealing that 20wt% and 40wt% AgI/BiVO₄ catalyzed this process more efficient than other AgI/BiVO₄ catalysts (Table 1, entries 14-19; Supporting Information, Table S1, entries 1-7). Considering the control of AgNO₃ (raw material for AgI/BiVO₄ catalyst) on account of its easy detonation, we chose the 20wt% AgI/BiVO₄ as target catalyst to perform the oxidative reaction. Subsequently, brief screening of the loadings of 20wt% AgI/BiVO₄ provided a satisfactory oxidation product yield using 15 mg 20wt% AgI/BiVO₄ (Table 1, entry 20). Increasing of the catalyst-loading to 20 or 25 mg did not further improve the product formation (Table 1, entries 21 and 22). Different reaction times were examined. Increase of reaction time to 16 h did not improve the product formation, and decrease of reaction time led to the decrease of the product yield (Table 1, entries 23-26). It was worth noting that acceptable product yield was obtained when the reaction was performed under air (Table 1, entry 27; Supporting Information, Table S1, entry 8). Finally, the optimized catalytic system was obtained, viz., 15 mg

20wt% AgI/BiVO₄ as catalyst, 2 mL H₂O as solvent, and O₂ balloon as oxidant under a 16 W white LED at 25 °C.

Table 1. Optimization of Reaction Conditions.

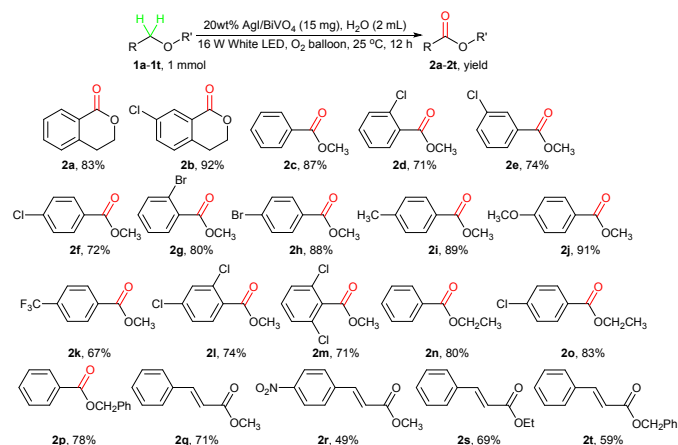


Entry	Cat. (mg)	Solvent	Yield ^a (%)
1	20wt% AgI/BiVO ₄ (10)	MeCN	28
2 ^b	20wt% AgI/BiVO ₄ (10)	MeCN	n. r.
3	-	MeCN	n. r.
4 ^c	20wt% AgI/BiVO ₄ (10)	MeCN	n. r.
5	20wt% AgI/BiVO ₄ (10)	H ₂ O	78
6	20wt% AgI/BiVO ₄ (10)	EtOH	35
7	20wt% AgI/BiVO ₄ (10)	MeOH	10
8	20wt% AgI/BiVO ₄ (10)	CH ₂ Cl ₂	16
9	20wt% AgI/BiVO ₄ (10)	Toluene	18
10	20wt% AgI/BiVO ₄ (10)	DMF	5
11	20wt% AgI/BiVO ₄ (10)	1,4-Dioxane	16
12	20wt% AgI/BiVO ₄ (10)	DCE	33
13	20wt% AgI/BiVO ₄ (10)	EA	n. r.
14	1wt% AgI/BiVO ₄ (10)	H ₂ O	10
15	5wt% AgI/BiVO ₄ (10)	H ₂ O	41
16	10wt% AgI/BiVO ₄ (10)	H ₂ O	66
17	40wt% AgI/BiVO ₄ (10)	H ₂ O	79
18	60wt% AgI/BiVO ₄ (10)	H ₂ O	67
19	80wt% AgI/BiVO ₄ (10)	H ₂ O	63
20	20wt% AgI/BiVO ₄ (15)	H ₂ O	83
21	20wt% AgI/BiVO ₄ (20)	H ₂ O	84
22	20wt% AgI/BiVO ₄ (25)	H ₂ O	81
23 ^d	20wt% AgI/BiVO ₄ (15)	H ₂ O	61
24 ^e	20wt% AgI/BiVO ₄ (15)	H ₂ O	75
25 ^f	20wt% AgI/BiVO ₄ (15)	H ₂ O	78
26 ^g	20wt% AgI/BiVO ₄ (15)	H ₂ O	82
27 ^h	20wt% AgI/BiVO ₄ (15)	H ₂ O	72

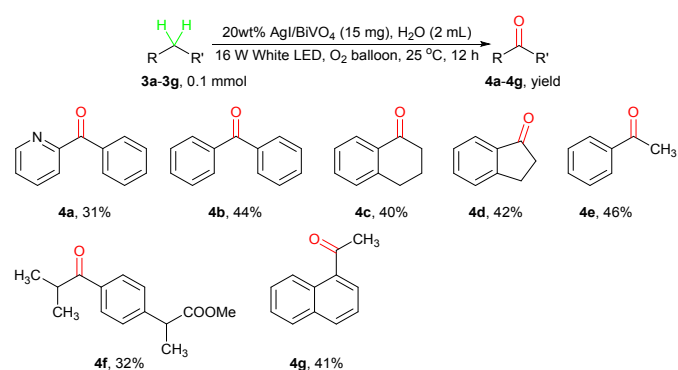
^aIsolated yield, n. r. = no reaction. ^bIn the dark. ^cUnder N₂ atmosphere. ^dReaction time was 6 h. ^eReaction time was 8 h. ^fReaction time was 10 h. ^gReaction time was 16 h. ^hThe oxidant is air (air balloon).

With the optimal conditions established, various ether compounds were investigated and the results were summarized in Scheme 2. Both electron-rich and electron-deficient ether compounds could be employed efficiently in this photocatalytic oxidation process, and good to excellent yields of the corresponding esters were obtained. We studied the direct oxidation of 7-chloroisochroman under this photocatalytic oxidation process affording the 7-chloroisochroman-1-one (**2b**) in 92% yield (Scheme 2, **2b**). Isochroman-1-one compounds were important structure found in a number of natural products and bioactive molecules. A good range of benzyl methyl ethers with *ortho*, *meta*, *para* or multi functional groups were well tolerated in this photocatalytic oxidation process (Scheme 2, **2c-2m**). Under the optimal conditions, benzyl methyl ether was converted into methyl benzoate (**2c**) in 87% yield (Scheme 2, **2c**). Chlorine substituent had slight influence on the oxidation reaction, and the yields of products decreased (Scheme 2, **2c-2f**). By comparison, substrates bearing bromine substituent

provided higher yields of methyl benzoates (Scheme 2, **2g** and **2h**). It might be due to the stronger electronegativity of chlorine. Substrates bearing methyl substituent and methoxy substituent followed similar trend, and afforded ester compounds in 89% and 91% yields, respectively (Scheme 2, **2i** and **2j**). The substrates which contained multiple chemically different C-H bonds oxidative positions were tested, and the sole products were benzoates (Scheme 2, **2a**, **2b** and **2i**). The electron-withdrawing group such as $-\text{CF}_3$ could afford the desired ester product in moderate yields (Scheme 2, **2k**). Ether bearing two substituents afforded the corresponding benzoates in good yields (Scheme 2, **2l** and **2m**). Benzyl ethyl ethers and benzyl ether were oxidized smoothly by this photocatalytic oxidation protocol, for example, benzyl ethyl ether, 1-chloro-4-(ethoxymethyl)benzene and benzyl ether underwent this protocol to afford ester products in 80%, 83% and 78% yields respectively (Scheme 2, **2n**, **2o** and **2p**). Interestingly, ethers containing carbon-carbon double bond which was sensitive to oxidation were transformed to the corresponding esters in 71%, 49%, 69% and 59% yields respectively (Scheme 2, **2q**, **2r**, **2s** and **2t**). The carbon-carbon double bond was left untouched.



Scheme 2. Selective Oxidation of Ether Compounds (isolated yield).

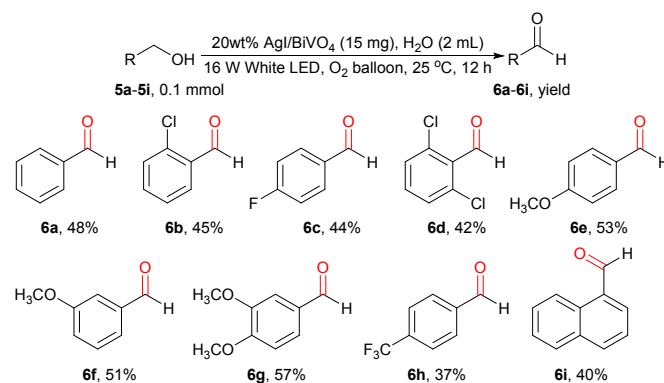


Scheme 3. Selective Oxidation of Alkylbenzenes (isolated yield).

Inspired by the reactivity of ether compounds, we subsequently studied the oxidation of alkylbenzenes with AgI/BiVO_4 and O_2 under a 16 W white LED at 25 °C for 12 h. When the dosage of alkylbenzenes were reduced to 0.1 mmol, alkylbenzenes could be oxidized to the corresponding ketone compounds in moderate yields (Scheme 3). It is worth

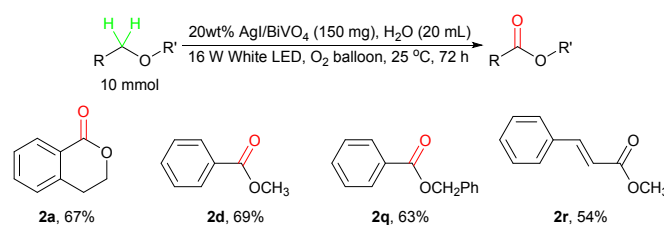
mentioning that the sp^3 C-H oxidation on ibuprofen methyl ester (drug molecule) occurred on the less hindered benzylic position with the formation of the ketone in 32% yield (Scheme 3, **4f**).

In organic chemistry, the oxidation of benzyl alcohols to the corresponding aromatic aldehydes using O_2 as oxidant is one of the most important transformations and of great significance both in theory and practice. When the dosage of benzyl alcohols were reduced to 0.1 mmol, the oxidation of benzyl alcohols was performed smoothly in our system with moderate yields of the corresponding aromatic aldehydes (Scheme 4).



Scheme 4. Selective Oxidation of Benzyl Alcohols (isolated yield).

To highlight the synthetic practicality of the present protocol, this sp^3 C-H oxidation methodology was evaluated on gram-scale (10 mmol). The desired products were obtained in good isolated yields (Scheme 5), indicating that this protocol was a practical process for the preparation of esters.



Scheme 5. Gram Scale Reactions (isolated yield).

Table 2. Leaching experiment and mercury poisoning experiments.

Entry	Reaction time	Yield ^a (%)
1	3 h	21
2	3 h + centrifugation + 9 h	20
3	3 h + mercury + 9 h	28
4	Catalyst + mercury, stirring for 3 h; then adding isochroman, 12 h	n. r.

^aIsolated yield, n. r. = no reaction.

The stability of the 20wt% AgI/BiVO_4 catalyst was certificated by the metal leaching test. The solid catalyst was removed by centrifugation at 3 h, and the reaction continued

for another 9 h. The yield of 1-isochromanone (**2a**) did not increase without 20wt% AgI/BiVO₄ catalyst (Table 2, entries 1 and 2). The results showed that this oxidation transformation was a heterogeneous catalytic system. Mercury can react with other metals forming alloys (amalgamation) or adsorb on other metal surface resulting in the deactivation of metal catalyst. This method is often used to detect whether the reaction occurs on the surface of metal particles. When mercury is added into the reaction system, the reaction is inhibited, indicating that the target reaction occurs on the surface of metal particles. The mercury poisoning experiments demonstrated this oxidation reaction occurred on the surface of the 20wt% AgI/BiVO₄ catalyst (Table 2, entries 1, 3 and 4).

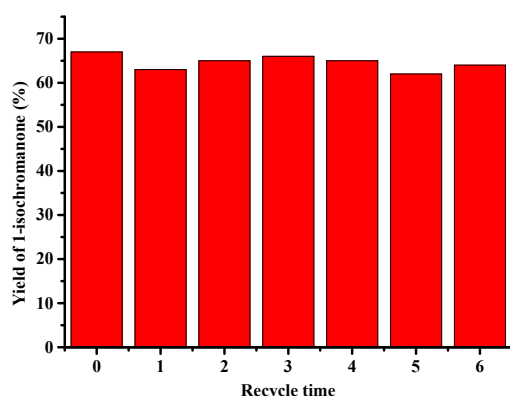


Figure 4. Recycle of 20wt% AgI/BiVO₄ for selective oxidation of isochroman. Reaction condition: isochroman (10 mmol), 20wt% AgI/BiVO₄ (150 mg), H₂O (20 mL), O₂ balloon, 16 W white LED, 25 °C, 72 h. Isolated yield after column chromatography.

As we known, recyclability for catalyst was an important and essential feature in large-scale catalytic reactions. The 20wt% AgI/BiVO₄ catalyst could be easily separated from the reaction mixture by centrifugation or filter, and then washed with ethanol three times and further reused after drying. In order to verify the reusability of 20wt% AgI/BiVO₄ catalyst, consecutive oxidation experiments were performed using isochroman as substrate on gram-scale under the optimized catalytic condition. Notably, the 20wt% AgI/BiVO₄ catalyst was successfully recycled up to six times without any significant loss of activity (Figure 4).

The yield of isochromanone (**2a**) was almost no change in the presence of UV cut-off filter which showed the oxidation reaction was irradiated by visible light (Table 3, entry 2). No product was produced in the absence of light or O₂ (Table 3, entries 3 and 4) which clearly showed the significance of light and O₂ in this reaction. Trace amount of 1-isochromanone (**2a**) was obtained when 15 mg BiVO₄ was used as catalyst (Table 3, entry 5). While low yield (28%) of 1-isochromanone (**2a**) was obtained in the cases of AgI (Table 3, entry 6), and a lower yield (12%) of 1-isochromanone (**2a**) was obtained when recycled AgI was used as catalyst (Table 3, entry 7) which might be because AgI was unstable under illumination. Furthermore, 1-isochromanone (**2a**) was obtained in 24% isolated yields in the presence of 3 mg AgI and 12 mg BiVO₄ (Table 3, entry 8) which was similar to the AgI-catalyzed result. These results illustrated AgI/BiVO₄ was not simple mixture of AgI and BiVO₄.

In the photocatalytic oxidation process, many reactive oxygen species, such as photogenerated holes (h⁺), superoxide radical anion (O₂^{•-}), hydroperoxyl radical (HOO[•]) or hydroxyl radicals (HO[•]), were supposed to be involved.^{14, 15} We conducted many quenching tests to recognize reactive oxidative species (Table 4). After adding 2,2,6,6-tetramethyl-1-piperidinyloxy (TEMPO), 2,6-di-*tert*-butyl-4-methylphenol (BHT) or 1,1-diphenylethylene (DPE) to the reaction mixture, no product was obtained which proved this photocatalytic oxidation process was radical pathway (Table 4, entries 1-6). Ammonium oxalate (AO), benzoquinone (BQ) and FeSO₄ acted as the scavengers for h⁺, O₂^{•-} and HOO[•] were introduced into the photocatalytic oxidation process, respectively. The results showed the presence of h⁺, O₂^{•-} and HOO[•] (Table 4, entries 7-10). Furthermore, addition of CuCl₂ to the oxidation mixture resulted in no reaction occur which clearly revealed the involvement of single electron transfer in the photocatalytic oxidation process (Table 4, entry 11).

Table 3. Control experiments.

Entry	Controlled parameter	Yield ^a (%)
1	Standard conditions	83
2	UV filter	84
3	In the dark	n. r.
4	Under N ₂ atmosphere	n. r.
5	Catalyst is BiVO ₄	Trace
6	Catalyst is AgI	28
7	Catalyst is recycled AgI	12
8	Catalyst is AgI (3 mg) + BiVO ₄ (12 mg)	24

^aIsolated yield, n. r. = no reaction. Standard conditions: isochroman (1 mmol), 20wt% AgI/BiVO₄ (15 mg), H₂O (2 mL), O₂ balloon, 16 W white LED, 25 °C, 12 h.

The electron paramagnetic resonance (EPR) measurements were performed to confirm the reactive oxygen species evolved in the photocatalytic oxidation process with 5, 5-dimethyl-1-pyrroline N-oxide (DMPO) as trapping reagent. As presented in Figure 5A, four obvious signals with 20wt% AgI/BiVO₄ in methanol were obtained which indicated the existence of DMPO-O₂^{•-} under visible light irradiation. This EPR spectra illustrated that the dissolved molecular oxygen on the surface of the AgI/BiVO₄ was reduced by photogenerated electrons to produce superoxide radical anion (O₂^{•-}). The characteristic quadruple peaks of DMPO-[•]OH were not displayed (Figure 5B). The hydroxyl radicals (HO[•]) may not be involved in the photocatalytic oxidation process which was good agreement with previous report.¹⁴ As shown in Figure 5C and 5D, DMPO-O₂^{•-} signals were also observed in the presence of pure AgI photocatalysts, whereas no corresponding signals were observed in the presence of pure BiVO₄ photocatalysts. These demonstrated that photogenerated electrons located on the conduction band (CB) of AgI could reduce O₂ to superoxide radical anion (O₂^{•-}) while those on the conduction band (CB) of BiVO₄ could not.¹⁶ According to the reports,¹⁴ the

photogenerated electrons on the CB of BiVO_4 could not reduce O_2 to produced superoxide radical anion ($\text{O}_2^{\cdot-}$), owing to the more positive edge potential of BiVO_4 (+0.46 eV) than that of $\text{O}_2/\text{O}_2^{\cdot-}$ (-0.33 eV vs NHE). The photogenerated electrons in the CB of AgI were transferred to O_2 absorbed on the surface of the AgI/ BiVO_4 and promoted superoxide radical anion ($\text{O}_2^{\cdot-}$) yields because the CB edge potential of AgI (-0.42 eV) was more negative than the standard redox potential E^0 ($\text{O}_2/\text{O}_2^{\cdot-}$) (-0.33 eV vs NHE).

Table 4. Quenching experiments.

Entry	Quenchers	Equivalents	Yield ^a (%)	Conclusions
1	TEMPO	0.5	n. r.	Radical
2	TEMPO	1.0	n. r.	Radical
3	BHT	0.5	n. r.	Radical
4	BHT	1.0	n. r.	Radical
5	DPE	0.5	n. r.	Radical
6	DPE	1.0	n. r.	Radical
7	AO	0.5	Trace	h^+
8	AO	1.0	Trace	h^+
9	BQ	1.0	Trace	$\text{O}_2^{\cdot-}$
10	FeSO_4	2.0	14	HOO^{\cdot}
11	CuCl_2	1.0	n. r.	SET

^aIsolated yield, n. r. = no reaction.

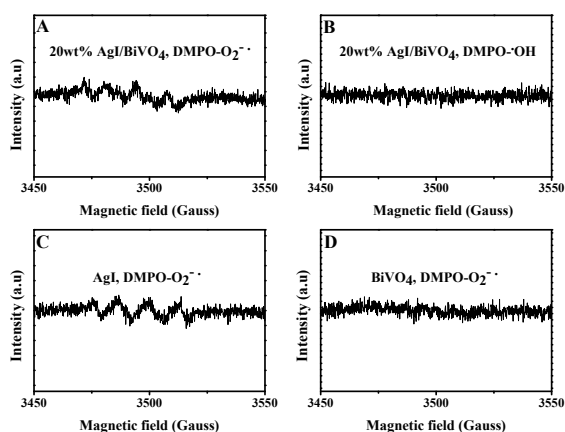


Figure 5. The EPR spectras of radical adducts trapped by DMPO spin-trapping under visible light irradiation for 10 min: (A) in methanol dispersion for $\text{DMPO-O}_2^{\cdot-}$ catalyzed by 20wt% AgI/ BiVO_4 ; (B) in aqueous dispersion for DMPO-OH catalyzed by 20wt% AgI/ BiVO_4 ; (C) in methanol dispersion for $\text{DMPO-O}_2^{\cdot-}$ catalyzed by AgI; (D) in methanol dispersion for $\text{DMPO-O}_2^{\cdot-}$ catalyzed by BiVO_4 .

The used 20wt% AgI/ BiVO_4 catalyst was characterized by XRD (Figure 6). The XRD pattern of the used 20wt% AgI/ BiVO_4 catalyst was compared with standard card of Ag (JCPDS No. 04-0782 and 41-1402) carefully, and no characteristic diffraction peaks of metallic Ag were observed, which illustrated that no AgI decomposed to Ag in the photocatalytic oxidation process.

On the basis of the above results and pertinent literatures, a possible Z-scheme mechanism for this photocatalytic oxidation process was proposed in Scheme 6. Under visible light, AgI and BiVO_4 were simultaneously excited, and electrons in valence band (VB) transferred to the conduction band (CB) forming

electron-hole pairs. The photogenerated electrons from the CB of BiVO_4 flowed into the VB of AgI. The transferred photogenerated electrons on the VB of AgI recombined with the holes there, which was faster than the recombination between e_{CB} - and h_{VB} + of AgI itself. A single electron transferred from ether to the VB of BiVO_4 , then generated cation radical **A**. The dissolved molecular oxygen on the surface of AgI/ BiVO_4 was reduced by the photogenerated electrons located on the CB of AgI to produce superoxide radical anion ($\text{O}_2^{\cdot-}$), which could then react with cation radical **A** to afford radical **B** and hydroperoxyl radical (HOO^{\cdot}). Radical **B** reacted with hydroperoxyl radical (HOO^{\cdot}) to generate the hydroperoxidate intermediate **C**.^{11a} The transformation from intermediate **C** to ester was supported by the Kornblum-type decomposition pathway.

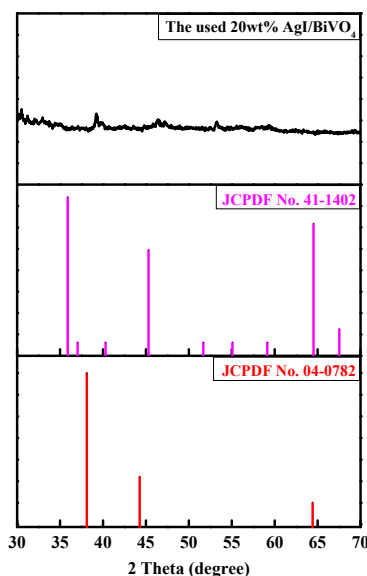
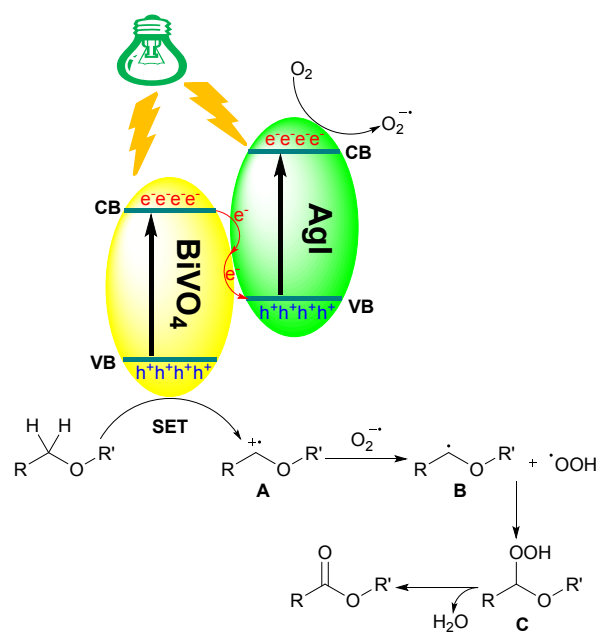


Figure 6. The XRD pattern of the used 20wt% AgI/ BiVO_4 .



Scheme 6. Possible Reaction Pathway.

Conclusions

In summary, we had developed an efficient method for oxidation of sp^3 C-H bonds to esters and ketones via a visible-light-induced process using AgI/BiVO₄ as photocatalyst and O₂ as oxidant in water. There were no hazardous oxidants, organic solvents, additives involved, thus, the oxidation process was environmentally friendly. The photocatalytic oxidation protocol exhibited a broad substrate scope and excellent regioselectivity. These AgI/BiVO₄ catalysts showed good reusability and were successfully recycled six times without any significant loss of activity. The synthetic utility of the photocatalytic oxidation protocol was demonstrated through gram-scale experiments. This photocatalytic oxidation protocol could also be used for the oxidation of benzyl alcohols to aromatic aldehydes. A plausible mechanism had been proposed. Further studies will be aimed at extending the scope of substrates, mass transfer of this catalytic system and further investigations into the reaction mechanism.

Conflicts of interest

There are no conflicts to declare.

Acknowledgements

We gratefully acknowledge the Research Foundation of Weifang Medical University, the Innovative Drug Research and Development Center of Weifang Medical University and the National Natural Science Foundation of China (No. 21773227) for support of this research.

Notes and references

- (a) Y. Zhang, W. Schilling and S. Das, *ChemSusChem* 2019, **12**, 2898. (b) L. Revathi, L. Ravindar, W. Y. Fang, K. P. Rakesh and H. L. Qin, *Adv. Synth. Catal.* 2018, **360**, 4652. (c) A. Savateev and M. Antonietti, *ACS Catal.* 2018, **8**, 9790.
- (a) L. Ren and S. Gao, *Chinese J. Org. Chem.* 2017, **37**, 1338. (b) L. Ren, L. Wang, Y. Lü, G. Li and S. Gao, *Chinese J. Catal.* 2016, **37**, 1216.
- Fe catalytic system: (a) B. Pieber and C. O. Kappe, *Green Chem.* 2013, **15**, 320. (b) S. J. Li and Y. G. Wang, *Tetrahedron Lett.* 2005, **46**, 8013.
- Cu catalytic system: (a) J. Liu, X. Zhang, H. Yi, C. Liu, R. Liu, H. Zhang, K. Zhuo and A. Lei, *Angew. Chem. Int. Ed.* 2015, **54**, 1261. (b) J. De Houwer, K. Abbaspour Tehrani and B. U. W. Maes, *Angew. Chem. Int. Ed.* 2012, **51**, 2745.
- Mn catalytic system: (a) H. Wang, L. Wang, S. Wang, X. Dong, J. Zhang and F. S. Xiao, *ChemCatChem* 2019, **11**, 401. (b) A. Shaabani, Z. Hezarkhani and E. Badali, *RSC Adv.* 2015, **5**, 61759. (c) T. K. M. Shing, Y. Y. Yeung and P. L. Su, *Org. Lett.* 2006, **8**, 3149.
- Co catalytic system: (a) D. P. Hruszkewycz, K. C. Miles, O. R. Thiel and S. S. Stahl, *Chem. Sci.* 2017, **8**, 1282. (b) S. M. Islam, K. Ghosh, R. A. Molla, A. S. Roy, N. Salam and M. A. Iqbal, *J. Organomet. Chem.* 2014, **774**, 61. (c) A. Shaabani, S. Keshipour, M. Hamidzad and S. Shaabani, *J. Mol. Catal. A Chem.* 2014, **395**, 494. (d) J. Q. Wang and L. N. He, *New J. Chem.* 2009, **33**, 1637. (e) A. Shaabani, E. Farhangi and A. Rahmati, *Appl. Catal. A Gen.* 2008, **338**, 14. (f) F. Minisci, C. Punta, F. Recupero, F. Fontana and G. Franco Pedulli, *J. Org. Chem.* 2002, **67**, 2671. DOI: 10.1039/C9GC03727F
- Pd catalytic system: G. Urgoitia, R. Sanmartin, M. T. Herrero and E. Domínguez, *Green Chem.* 2011, **13**, 2161.
- Bimetallic catalytic system: (a) J. Luo, K. Xuan, Y. Wang, F. Li, F. Wang, Y. Pu, L. Li, N. Zhao and F. Xiao, *New J. Chem.* 2019, **43**, 8428. (b) H. Wang, L. Wang, J. Zhang, C. Wang, Z. Liu, X. Gao, X. Meng, S. J. Yoo, J. G. Kim, W. Zhang and F. S. Xiao, *ChemSusChem* 2018, **11**, 3965. (c) S. Fan, W. Dong, X. Huang, H. Gao, J. Wang, Z. Jin, J. Tang and G. Wang, *ACS Catal.* 2017, **7**, 243.
- Non-metal catalytic system: (a) L. Wang, Y. Zhang, R. Du, H. Yuan, Y. Wang, J. Yao and H. Li, *ChemCatChem* 2019, **11**, 2260. (b) K. J. Liu, Z. H. Duan, X. L. Zeng, M. Sun, Z. L. Tang, S. Jiang, Z. Cao and W. M. He, *ACS Sustain. Chem. Eng.* 2019, **7**, 10293. (c) F. Yang, B. Zhou, P. Chen, D. Zou, Q. Luo, W. Ren, L. Li, L. Fan and J. Li, *Molecules* 2018, **23**, 1922. (d) H. Zhang, Y. Wang, L. Huang, L. Zhu, Y. Feng, Y. Lu, Q. Zhao, X. Wang and Z. Wang, *Chem. Commun.* 2018, **54**, 8265. (e) Y. Zhang, Y. Yue, X. Wang, K. Wang, Y. Lou, M. Yao, K. Zhuo, Q. Lv and J. Liu, *Asian J. Org. Chem.* 2018, **7**, 2459. (f) Z. Zhang, Y. Gao, Y. Liu, J. Li, H. Xie, H. Li and W. Wang, *Org. Lett.* 2015, **17**, 5492. (g) J. Ma, Z. Hu, M. Li, W. Zhao, X. Hu, W. Mo, B. Hu, N. Sun and Z. Shen, *Tetrahedron* 2015, **71**, 6733. (h) L. Ren, L. Wang, Y. Lv, G. Li and S. Gao, *Org. Lett.* 2015, **17**, 2078. (i) H. Kawabata and M. Hayashi, *Tetrahedron Lett.* 2004, **45**, 5457.
- (a) X. Zhang, K. P. Rakesh, L. Ravindar and H. L. Qin, *Green Chem.* 2018, **20**, 4790. (b) X. Y. Wang, Z. P. Shang, G. F. Zha, X. Q. Chen, S. N. A. Bukhari and H. L. Qin, *Tetrahedron Lett.* 2016, **57**, 5628.
- (a) K. C. C. Aganda, B. Hong and A. Lee, *Adv. Synth. Catal.* 2019, **361**, 1124. (b) G. Zhao, B. Hul, G. W. Busser, B. Peng and M. Muhler, *ChemSusChem* 2019, **12**, 2795. (c) D. Pan, Y. Wang, M. Li, X. Hu, N. Sun, L. Jin, B. Hu and Z. Shen, *Synlett*, 2019, **30**, 218. (d) L. C. Finney, L. J. Mitchell and C. J. Moody, *Green Chem.* 2018, **20**, 2242. (e) Y. Zhang, D. Riemer, W. Schilling, J. Kollmann and S. Das, *ACS Catal.* 2018, **8**, 6659. (f) L. Ren, M. M. Yang, C. H. Tung, L. Z. Wu and H. Cong, *ACS Catal.* 2017, **7**, 8134. (g) S. Tripathi, S. N. Singh and L. D. S. Yadav, *RSC Adv.* 2016, **6**, 14547. (h) F. Rusch, J. C. Schober and M. Brasholz, *ChemCatChem* 2016, **8**, 2881. (i) B. Mühldorf and R. Wolf, *Angew. Chem. Int. Ed.* 2016, **55**, 427. (j) H. Yi, C. Bian, X. Hu, L. Niu and A. Lei, *Chem. Commun.* 2015, **51**, 14046. (k) I. Itoh, Y. Matsusaki, A. Fujiya, N. Tada, T. Miura and A. Itoh, *Tetrahedron Lett.* 2014, **55**, 3160. (l) M. Kojima, K. Oisaki and M. Kanai, *Tetrahedron Lett.* 2014, **55**, 4736. (m) P. Zhang, Y. Wang, J. Yao, C. Wang, C. Yan, M. Antonietti and H. Li, *Adv. Synth. Catal.* 2011, **353**, 1447.
- L. Ren, L. Wang, Y. Lv, S. Shang, B. Chen and S. Gao, *Green Chem.* 2015, **17**, 2369.
- Z. Xiang, Y. Wang, P. Ju, Y. Long and D. Zhang, *J. Alloys Compd.* 2017, **721**, 622.
- F. Chen, Q. Yang, J. Sun, F. Yao, S. Wang, Y. Wang, X. Wang, X. Li, C. Niu, D. Wang and G. Zeng, *ACS Appl. Mater. Interfaces* 2016, **8**, 32887.
- X. Liu, F. Huang, Y. Yu, P. Zhao, Y. Zhou, Y. He, Y. Xu and Y. Zhang, *Appl. Catal. B Environ.* 2019, **253**, 149.
- X. Wang, J. Yang, S. Ma, D. Zhao, J. Dai and D. Zhang, *Catal. Sci. Technol.* 2015, **6**, 243.